Free Radical Biology and Medicine 89 (2015) 1067–1076

Contents lists available at ScienceDirect

Free Radical Biology and Medicine

journal homepage: www.elsevier.com/locate/freeradbiomed

Original Contribution

The molecular mechanism behind reactive aldehyde action on transmembrane translocations of proton and potassium ions

Olga Jovanovic [a], Alina A. Pashkovskaya [a], Andrea Annibal [b], Mario Vazdar [c], Nadine Burchardt [a], Anna Sansone [d], Lars Gille [e], Maria Fedorova [b], Carla Ferreri [d], Elena E. Pohl [a,*]

[a] Institute of Physiology, Pathophysiology and Biophysics, University of Veterinary Medicine, Vienna, Austria
[b] Institute of Bioanalytical Chemistry, Faculty of Chemistry and Mineralogy, Center for Biotechnology and Biomedicine, University of Leipzig, Germany
[c] Division of Organic Chemistry and Biochemistry, Rudjer Boskovic Institute, Zagreb, Croatia
[d] ISOF, Consiglio Nazionale delle Ricerche, Bologna, Italy
[e] Institute of Pharmacology and Toxicology, University of Veterinary Medicine, Vienna, Austria

ARTICLE INFO

Article history:
Received 28 August 2015
Received in revised form
24 October 2015
Accepted 26 October 2015
Available online 28 October 2015

Keywords:
Mitochondrial proteins
Valinomycin
CCCP
Phosphatidylethanolamine
Membrane lipids
Planar bilayer membranes
Membrane conductance
Membrane order parameter
Boundary potential
Surface potential
Phloretin
PE-adducts
HNE-adducts
Schiff bases
Michael adducts
Transporters

ABSTRACT

Membrane transporters are involved in enormous number of physiological and pathological processes. Under oxidative stress they become targets for reactive oxygen species and its derivatives which cause protein damage and/or influence protein function(s). The molecular mechanisms of this interaction are poorly understood. Here we describe a novel lipid-mediated mechanism by which biologically important reactive aldehydes (RAs; 4-hydroxy-2-nonenal, 4-hydroxy-2-hexenal and 4-oxo-2-nonenal) modify the activity of several membrane transporters. We revealed that investigated RAs covalently modify the membrane lipid phosphatidylethanolamine (PE), that lead to the formation of different membrane active adducts. Molecular dynamic simulations suggested that anchoring of PE-RA adducts in the lipid head-group region is primarily responsible for changes in the lipid membrane properties, such as membrane order parameter, boundary potential and membrane curvature. These caused the alteration of transport activity of mitochondrial uncoupling protein 1, potassium carrier valinomycin and ionophore CCCP. In contrast, neither direct protein modification by RAs as previously shown for cytosolic proteins, nor its insertion into membrane bilayers influenced the studied transporters. Our results explain the diversity of aldehyde action on cell proteins and open a new field in the investigation of lipid-mediated effects of biologically important RAs on membrane receptors, channels and transporters.

1. Introduction

Mitochondria produce a substantial amount of superoxide anion $O_2^{\bullet -}$, which is able to give rise to other reactive species, among them reactive aldehydes, such as 4-hydroxy-2-nonenal (HNE), 4-oxo-2-nonenal (ONE) and 4-hydroxy-2-hexenal (HHE) [1]. Whereas HNE and ONE are peroxidation products derived from n-6 polyunsaturated fatty acids (PUFA), like arachidonic or linoleic acid, HHE is a peroxidation product of n-3 PUFAs [2]. These aldehydes are much more stable than ROS; their non-charged structure enables them to move far from their place of origin to target proteins, DNA and phospholipids [3–7]. HNE, the most intensively studied aldehyde, was found in different tissues and blood plasma. At low concentrations, HNE is involved in signaling processes, cell proliferation, differentiation and apoptosis [8]. At high concentrations HNE is toxic and was reported to be involved in the pathogenesis of many diseases [9]. The molecular mechanisms

Abbreviations: RA, reactive aldehydes; ONE, 4-oxo-2-nonenal; HNE, 4-hydroxy-2-nonenal; HHE, 4-hydroxy-2-hexenal; UCP1, uncoupling protein 1; CCCP, carbonyl cyanide m-chlorophenyl hydrazine; AA, arachidonic acid; DHA, docosahexaenoic acid; EPA, eicosapentanoic acid; ROS, reactive oxygen species; FA, long chain fatty acid; DOPE, 1,2-Dioleoyl-sn-glycero-3-phosphoethanolamine; DOPC, 1,2-dioleoyl-sn-glycero-3-phosphocholine; CL, cardiolipin; PG, phosphatidylglycerol; DPPC, 1,2-dihexadecanoyl-sn-glycero-3-phosphocholine

* Corresponding author.
E-mail address: elena.pohl@vetmeduni.ac.at (E.E. Pohl).

http://dx.doi.org/10.1016/j.freeradbiomed.2015.10.422

responsible for such a variety of HNE effects are poorly understood. An emerging body of evidence shows that not only HNE, but also other biologically active aldehydes mediate non-enzymatic post-translational protein modifications by formation of adducts with several amino acids such as cysteine, lysine, histidine and, in case of ONE, arginine [6,10–12]. Few reports demonstrate the ability of RA to form adducts with aminophospholipids, such as phosphatidylethanolamine (PE) [13,14]. The consequences of RA-PE adduct formation on the function of membrane proteins have thus far been poorly studied.

Uncoupling proteins – membrane proteins that belong to the superfamily of mitochondrial anion transporters – have been controversially discussed as to whether they regulate ROS and as negative feedback are regulated by ROS and their derivatives [5,15,16]. In our previous work, we demonstrated that although HNE did not influence the activity of the protein directly, it strongly potentiated the UCP-mediated proton transport in the presence of fatty acids [5]. We first hypothesized that HNE binding to Cys, Lys and His residues of protein induces a conformational change of UCP1 that leads to the strong potentiation of its activity. However, although UCP1, with its 7 cysteine, 17 lysine and 3 histidine residues represents a good target for aldehyde action, blocking the afore-mentioned amino acids did not lead to complete inhibition of the HNE-effects. This knowledge led us to the current hypothesis that the molecular mechanism may rather entail covalent modification of the aminophospholipids, which then leads to the alteration of the lipid membrane parameters [17] and to the facilitation of fatty acids transport mediated by uncoupling proteins.

In this work, we therefore compared the effect of biologically important reactive aldehydes (HNE, ONE and HHE) which have similar structures, but are known for their different activity *in vivo*, on UCP1, valinomycin and CCCP transport function. By comparing the three aldehydes, we aimed to reveal (i) whether the RA-mediated modulation of protein activity is mediated by a lipid environment rather than by direct interaction between aldehyde and protein, and (ii) whether definite structural differences lead to different aldehyde reactivity.

2. Materials and methods

2.1. Chemicals

Hexane, hexadecane, Na_2SO_4, MES, TRIS, EGTA, ammonium formiate, 5-doxyl stearic acid, DOPC, DOPE, cardiolipin and arachidonic acid were purchased from Sigma Aldrich GmbH (Germany). ONE, HNE and HHE came from Cayman Chemicals. *E. coli* polar lipid and DPhPC, were purchased from Avanti polar lipids. ULC/MS grade methanol was supplied by Biosolve BV (Valkenswaard, Netherlands). Chloroform was from Merck KGaA (Darmstadt, Germany).

2.2. Reconstitution of UCP1 in liposomes

The recombinant uncoupling protein (mUCP1) was purified from *E. coli* inclusion bodies and reconstituted into liposomes as previously described [18]. The free fatty acid (arachidonic acid (AA), 20:4, n-6) at a concentration of 15 mol% was directly added to the lipid phase before membrane formation. RAs were directly added to the buffer solution.

2.3. Formation and measurements of planar membrane electrical parameters

Planar lipid bilayers were formed from proteoliposomes or liposomes on the tip of plastic pipettes as previously described [18]. Membrane formation and bilayer quality was monitored by capacitance measurements ($0.72 \pm 0.05\ \mu F/cm^2$). The capacitance neither depends on protein nor on fatty acid or reactive aldehydes (RA) content. Current–voltage (*I–V*) characteristics were measured by a patch-clamp amplifier (EPC 10, HEKA Elektronik Dr. Schulze GmbH, Germany). Total membrane conductance was calculated from a linear fit of experimental data (I) at applied voltages in the range of -50 mV to 50 mV as previously described [17]. For this study, liposomes and proteoliposomes were subsequently incubated with different concentrations of each RA for 15 min at 32 °C.

2.4. Preparation of liposomes and measurement of Zeta-potential

For liposome formation, lipids (DOPC and DOPE) were mixed in the required ratio, the solvent (chloroform) was removed by evaporation and an appropriate volume of buffer (50 mM Na_2SO_4, 10 mM TRIS, 10 mM MES, 0.6 mM EGTA) was added to reach the final lipid concentration of 0.2 mg/ml. Unilamellar vesicles were obtained using a small-volume extruder (Avanti Polar lipids Inc.) with a 100 nm filter. The liposomes were incubated with each RA at a concentration of 0.5 mM for 15 min at RT. Measurements of the electrophoretic mobility of liposomes in an electrical field were performed by a Malvern Zetasizer Nano ZS device (Malvern, UK) at 25 °C and pH 7.32. The obtained velocity data were used for the calculation of electrophoretic mobility of liposomes. The Smoluchowski model was applied to calculate the Zeta-potential.

2.5. Determination of order parameters in lipid bilayers using the Electron Paramagnetic Resonance (EPR) method

The order parameter of the lipid bilayer was determined by inserting 5-doxyl stearic acid spin label (5-DSA) (7.5 nmol/mg lipid) into liposomes (5 mg lipid/ml) in the presence of 0.5 mM RAs and/or respective solvents, if required. EPR measurements and calculation of order parameters were performed as previously described [5].

2.6. Analysis of fatty acid residues by gas spectrometry

Unilamellar liposomes (3 mg/ml) made from *E. coli* polar lipids with or without AA, were incubated with HNE, ONE or HHE for 30 min. The phospholipid extraction and analysis of the fatty acid tails was performed as described previously [19]. In brief, treatment with 0.5 M KOH/MeOH at room temperature converted the fatty acid residues of the phospholipids into their corresponding fatty acid methyl esters (FAME). FAMEs were then extracted with n-hexane and analyzed by GC. Fatty acids were identified by comparison with standard references.

2.7. Mass spectrometric analysis of modified lipid vesicles

Aldehyde-treated lipid vesicles were mixed with chloroform: methanol (1:1; v/v), an organic phase containing modified lipids was separated by centrifugation (4000 g, 10 min, RT), diluted 1:5 (v/v) in ESI solution (methanol: chloroform (2:1; v/v) containing 5 mmol/L ammonium formate) and directly analyzed by direct injection using robotic nanoflow ion source TriVersa NanoMate (AdvionBio Sciences, Ithaca NY) equipped with nanoelectrospray chips (1.5 kV ionization voltage, 0.4 psi back pressure) coupled to a LTQ Orbitrap XL ETD mass spectrometer (Thermo Fischer Scientific GmbH, Bremen, Germany). The temperature of the transfer capillary was set to 200 °C and the tube lens voltage to 115 V. Mass spectra were recorded from *m/z* 400 to 2000 in the Orbitrap mass analyzer at a mass resolution of 100,000 at *m/z* 400. Tandem mass spectra were acquired by performing CID (isolation width 1–1.5 u,

normalized collision energy 25–30%, activation time 30 ms, activation Q 0.25) in the linear ion trap. Data were acquired and analyzed using Xcalibur software (version 2.0.7, Thermo Fisher Scientific, San Jose, CA, USA). All MS/MS spectra were manually annotated.

2.8. Molecular dynamics (MD) simulations

Molecular dynamics (MD) simulations of lipid bilayer membranes were performed in aqueous solutions as closely as possible to match experimental conditions. However, due to the lack of available force field parameters, the 1,2-Dioleoyl-sn-glycero-3-phosphocholine (DOPC) bilayer used in the experiments was replaced by a 1,2-dipalmitoyl-sn-glycero-3-phosphocholine (DPPC) bilayer while cardiolipin was not included in simulations. DPPC, 4-hydroxynonenal (HNE), 4-oxononenal (ONE), Michael-HNE adduct, Schiff-HNE adduct and Schiff-ONE adduct were described with SLipids [20–22] and CHARMM [22–24] force field. All missing bonding and nonbonding parameters of HNE, ONE and adduct molecules in the existing Slipids force field were updated with compatible CHARMM36 parameters while atomic charges were calculated by the Merz-Singh–Kollman scheme [25] which consisted of B3LYP/6-31G(d) geometry optimization of the molecule of interest and subsequent single point ESP charge calculation using B3LYP/cc-pVTZ method.

Bilayers containing 128 lipid molecules were constructed by placing individual lipids on an 8×8 grid resulting in a bilayer of two monolayers, each containing 64 individual lipid molecules (Table S2). In the case of mixed bilayers, HNE, ONE and adduct molecules, respectively, were randomly placed in each of the leaflets replacing the same number of DPPC molecules. Lipid bilayer membranes were equilibrated until a constant area per lipid was obtained (i.e., at least 100 ns for DPPC bilayers and 200 ns for all other bilayers). All systems were placed in a unit cell and solvated by ca. 11,000 water molecules using the TIP3P water model [24]. The size of the unit cell was approximately $6.5 \times 6.5 \times 12.0\ \mathrm{nm}^3$. The system was set up so that the lipid bilayer spanned the *xy* plane and the *z* coordinate was normal to the bilayer. 3D periodic boundary conditions were employed with long-range electrostatic interactions beyond the non-bonded cut-off of 1 nm. This accounted for using the particle-mesh Ewald procedure [26] with a Fourier spacing of 1.2 nm. The real space Coulomb interactions were cut off at 1 nm, while van der Waals interactions were cut-off at 1.4 nm. Simulations were performed with semi-isotropic pressure coupling, independently, in the directions parallel and perpendicular to the bilayer normal, employing the Parrinello–Rahman algorithm [27]. The pressure was set to 1 bar and a coupling constant of $10\ \mathrm{ps}^{-1}$ was employed. Two temperatures were used for simulations – 310 K (which closely matched an experimental temperature of 305 K) and 323 K (which is sufficiently above phase transition temperature of DPPC lipid) and independently controlled with the Nose–Hoover thermostat [28] for the lipid water sub-systems, with a coupling constant of $0.5\ \mathrm{ps}^{-1}$. Bond lengths within the simulated molecules were constrained using the LINCS algorithm [29]. Water bond lengths were kept constant employing the SETTLE method [30]. Equations of motion were integrated using the leap-frog algorithm with a time step of 2 fs. All the simulated systems were equilibrated for at least 100 ns, depending on the system, with a subsequent 100 ns simulation time used for analysis. MD simulations were performed with the GROMACS program package, version 4.5.4 [31] while quantum chemical calculations were performed using Gaussian 09 [32].

2.9. Statistical analysis

Data are presented as mean values ± SD. Statistical significance was determined using Student's *t*-test.

3. Results

3.1. Effect of ONE, HNE and HHE on UCP1 reconstituted in bilayer membranes of various lipid compositions

We have previously shown that 4-hydroxy-2-nonenal (HNE) only activates inner membrane mitochondrial uncoupling proteins 1 and 2 (UCP1 and UCP2) in the presence of fatty acids [5]. To reveal whether other biologically important reactive aldehydes (RA) can directly influence protein activity and whether the chemical structure of aldehyde is important for the magnitude of the effect, we have now investigated 4-hydroxy-2E-hexenal ($C_6H_{10}O_2$, HHE), which has a shorter backbone than HNE, and 4-oxo-2-nonenal ($C_9H_{14}O_2$, ONE), which has the same length, but has a carbonyl instead of a hydroxyl group at C4 (Fig. 1a). For this purpose, we reconstituted UCP1 in artificial bilayer membranes made from *E. coli* polar lipids and compared relative conductances G/G_0 of FA-free and FA-containing membranes in the presence (G) and absence (G_0) of different RAs. Conductance (G) was determined at 0 mV from current–voltage (I–V) characteristics, which were linear in the range of −50 to 50 mV (Fig. S1). *E. coli* polar lipid extract which contained phosphatidylethanolamine, phosphatidylglycerol and cardiolipin (PE:PG:CL = 71.4:23.4:5.2, in mol%) respectively, shows that both HHE and ONE, as similar to HNE, cannot directly activate UCP1 (Fig. 1b, inset). Comparison of G/G_0 for investigated aldehydes shows a concentration-dependent increase of activation potential in this order: HHE«HNE < ONE over the whole concentration range (90–800 μM, Fig. 1b). The much lower hydrophobicity of HHE, which is three C-atoms shorter than HNE, could be the most likely explanation for its smaller influence on membrane conductance. Although aldehyde concentrations used in this study are higher than those typically reported as non-toxic in cells, the lack of a proton leak in the lipid membrane without PE ensured that RA concentrations used in our system were not toxic. It is worth mentioning that local aldehyde concentrations (for example in the vicinity of the membrane) can be higher than reported for the whole cell or tissue.

To investigate whether the membrane lipid composition influences the aldehyde activation potential in membranes reconstituted with FA and UCP1, we further compared membranes containing DOPE:DOPC:CL and DOPC:CL as a model for an inner mitochondrial membrane and as a "PE-knockout" model, respectively. Fig. 1c shows that G_0 does not depend on lipid composition of the membrane that has only been reconstituted with protein (white bars). The addition of HNE or ONE only significantly increased G in this order $G(\mathrm{ONE}) > G(\mathrm{HNE})$ in bilayers which contained DOPE. In contrast, we observed no effect from both aldehydes if membranes were made from DOPC and CL (Fig. 1c).

3.2. Investigation of valinomycin–aldehyde interaction in planar bilayer membranes of different lipid compositions

To test whether the presence of PE is a common requirement for aldehyde action on the transmembrane transport, we reconstituted lipid bilayer membranes with dodecadepsipeptide antibiotic valinomycin (0.05–0.1 μM) which is known to transport potassium across a membrane. Fig. 1d (empty dots) demonstrates that again, no increase in conductance was measured in the absence of PE. The relative membrane current increase, I/I_0, in the presence of PE was dependent on aldehyde concentration. The

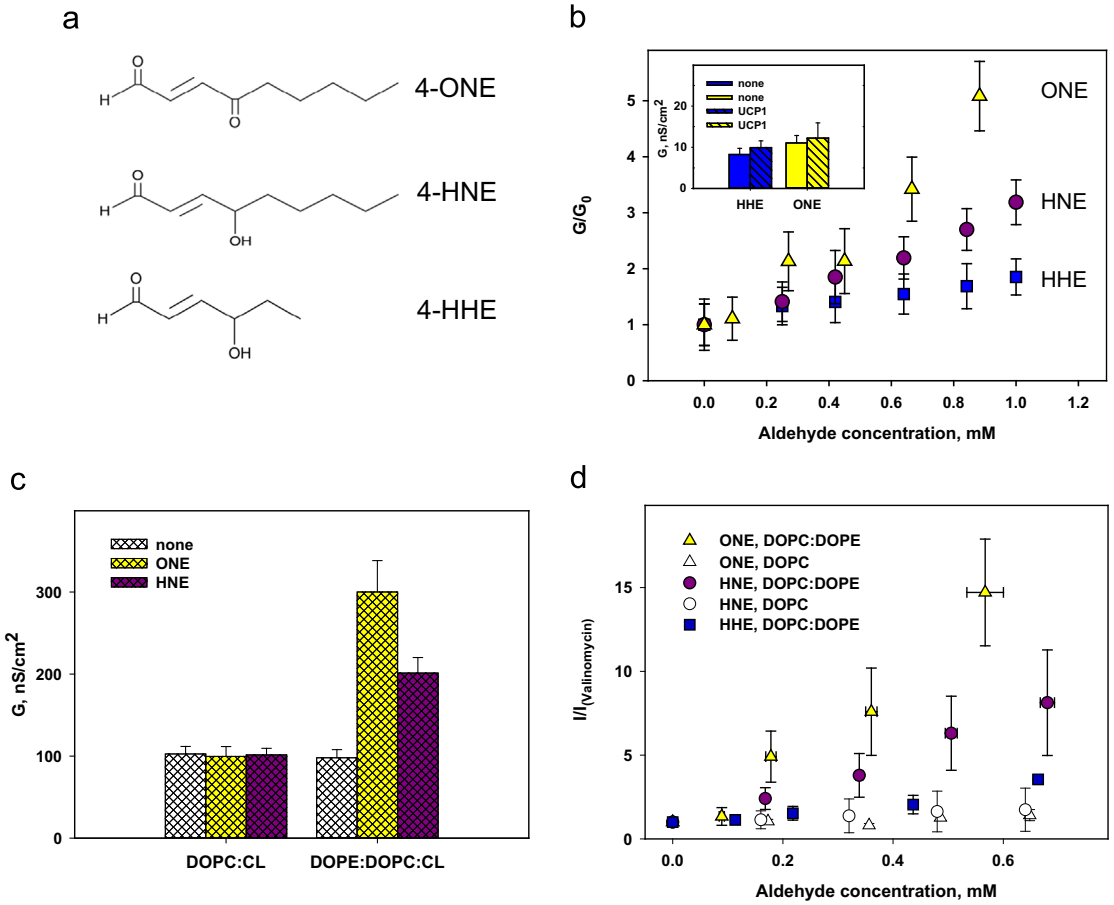

Fig. 1. Measurements of electrophysiological parameters of the bilayer membrane in the presence of different reactive aldehydes. (a) Schematic presentation of α, β-unsaturated aldehydes used in the study. (b) Dependence of UCP-mediated membrane conductance, *G*, on RAs concentration. Lipid bilayer membranes were made from *E. coli* lipids reconstituted with UCP1 and arachidonic acid (AA). The concentrations of lipid, UCP1 and AA were 1.5 mg/ml, 10 μg/(mg of lipid) and 15 mol% respectively. G_0 is conductance of FA activated UCP1 in the absence of RA. Insert. The effect of HHE (blue bars) and ONE (yellow bars) on the total membrane conductance G in the absence (empty bars) and presence of UCP1 (dashed bars). Concentrations of HHE and ONE were 0.84 mM and 0.88 mM, respectively. (c) Influence of the membrane lipid composition on the activation of UCP1 in the presence of AA and RAs. Differently colored bars indicate FA activated UCP1 without RAs (white), in the presence of ONE (yellow) and HNE (violet). Concentrations of lipid and UCP1 were 1.5 mg/ml and 5.3 μm/(mg lipid) respectively. Membrane lipid composition was DOPC:CL=90:10 and DOPE:DOPC:CL=33:57:10 mol%. The buffer solution in all experiments contained 50 mM Na_2SO_4, 10 mM TRIS, 10 mM MES, 0.6 mM EGTA at pH 7.35 and T=32 °C. (d) Dependence of valinomycin-mediated membrane current, I, on RAs' concentration in lipid bilayer membranes composed of different lipids. $I_{(valinomycin)}$ is a current measured in membranes reconstituted only with valinomycin. Membranes were made from DOPE: DOPC (30:70 mol%, colored symbols) or from 100% DOPC (empty symbols). Valinomycin was added to both compartments in a concentration of 0.05–0.1 μM. Buffer solution contained 50 mM KCl, 10 mM Tris, 10 mM MES, at pH 7.4 and T=24 °C. Data points represent means and standard deviation from 3–5 independent experiments. (For interpretation of the references to color in this figure legend, the reader is referred to the web version of this article.)

activity of aldehydes has shown a pattern similar to that which was measured with UCP1: ONE > HNE»HHE (Fig. 1d, colored dots).

3.3. *Modifications of DOPE head group by reactive aldehydes*

Reactive aldehydes are known to form different adducts such as the Michael adduct, Schiff base and pyrrole derivative with amino acids [33] and aminophospholipids [13,34]. To reveal which adducts were formed by each aldehyde studied in our system, we used high resolution mass spectrometry (MS) on ESI-Orbitrap. Protonated ions of unmodified DOPE and DOPC were detected at *m/z* 744.55 and 786.60, respectively (Fig. 2a). After incubation of lipid vesicles with HNE, several new ions were observed at *m/z* 882.65, 900.67, 1020.76 and 1056.78 (Fig. 2b–d). Based on the high accuracy of the Orbitrap mass analyzer, elemental compositions for new compounds were assigned and structures of DOPE-HNE adducts were proposed (Fig. 2e; Table S1). Proposed structures were further confirmed using consecutive tandem mass spectrometry experiments in a linear ion trap. CID MSn analysis allowed identification of single and double Schiff bases and Michael adducts of HNE on a nucleophilic amino group of DOPE (Figs. S2–S5). As illustrated in Fig. 2b, the most intensive product obtained by co-incubation of lipid vesicles with HNE corresponded to the Michael adduct at *m/z* 900.67. Intensities of Schiff base, double Schiff base and double Michael adducts were at least one order of magnitude lower than the intensity of the single Michael adduct (however it was still possible to perform MS^3 experiments illustrated in Supplementary Information). Indeed, it was shown by numerous studies that Michael adducts formed by HNE with nucleophilic substrates can undergo cyclization with formation of hemiacetals (will have the same mass increment of 156 u) which can be further dehydrated (mass increment of 138 u). Thus an adduct at *m/z* 882.65 may in part correspond not only to the Schiff base, but also to the dehydrated hemiacetal. Schiff base adducts between HNE and primary amines are also known to undergo cyclization with formation of a pentylpyrrole derivative accompanied by the loss of water. In the case of an HNE reaction with DOPE, the product would have *m/z* value 864.6. However, the ion at this *m/z* was not detected under conditions used in this experiment. Furthermore, the formation of double and even triple

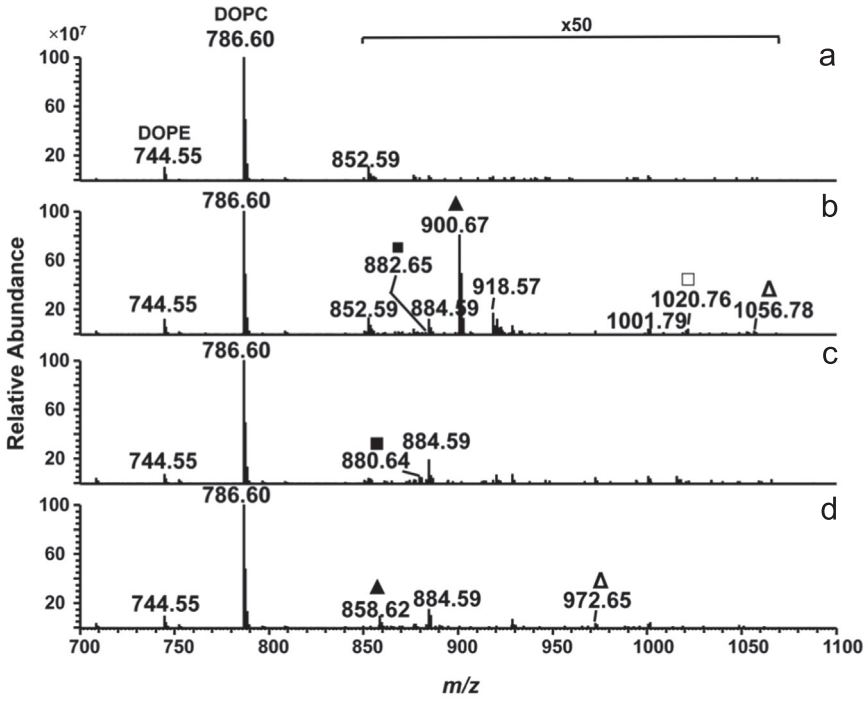

e

	HNE-PE adduct (B)	ONE-PE adduct (C)	HHE-PE adduct (D)
Michael adduct (MA)	900.67		858.62
Schiff base adduct (SB)	882.65	880.64	
Double MA	1056.78		972.65
Double SB adduct	1020.76		

Fig. 2. ESI-Orbitrap MS spectra of RA-modified lipid vesicles. Lipid vesicles made of DOPE:DOPC:CL with a molar ratio of 45:45:10 mol% were incubated without aldehydes (a), with HNE (b), ONE (c), and HHE (d). ■ indicate Schiff base adduct, ▲ Michael adduct, □ double Schiff base adduct, and Δ double Michael adduct. (e) Covalent modifications of PE by RAs. Proposed structures of HNE-, ONE- and HHE-modified DOPE based on mass spectrometry data.

adducts between primary amine of PE head group and saturated aldehydes was demonstrated previously *in vitro* [35].

Incubation of lipid vesicles with ONE resulted in the formation of single Schiff bases which were detected at *m*/*z* 800.64 (Fig. 2c; Fig. S6). Neither double Schiff bases nor double Michael adducts were detected. HHE-DOPE co-incubation resulted in two new compounds detected at *m*/*z* 858.62 and 972.65 (Fig. 2d) which were assigned to single and double Michael adducts of HHE to the amino group of PE based on elemental composition (Table S1). The structure of adducts was further confirmed in MSn experiments (Figs. S7 and S8). Previously, we reported the formation of dimeric and even trimeric adducts of reactive aldehydes (alkenals) with the nucleophilic head group of PE lipids [35]. We demonstrated that after the first Schiff base was formed, the addition of a second molecule of aldehyde occurred via β-aldol condensation between β-carbon (C2) atom of a first aldehyde and the carbonyl group of a

second aldehyde molecule. Formation of hemiacetals between the hydroxyl group in position C4 of the first α,β-unsaturated aldehyde and a carbonyl group of a second aldehyde molecule were proposed for double Michael adducts (Fig. 2e).

To confirm that the RAs we used only interacted with an amine group of DOPE, we performed GC–MS analysis of DOPE:DOPC:CL, DOPC:CL and *E. coli* polar lipid samples in the presence of aldehydes (Fig. S9a, c and e) and in the presence of aldehydes and arachidonic acid (Fig. S9b, d and f). In none of the cases was modification of PE-esterified fatty acids or AA acyl chains found.

3.4. Measurements of lipid membrane parameters in the presence of aldehydes

To understand how aldehyde-PE adducts influence the activity of membrane proteins/peptides, we compared different lipid membrane parameters such as boundary potential, surface potential and membrane order parameter in the presence of three aldehydes.

First, we measured the membrane conductance in the presence of potassium ionophore valinomycin (0.05–0.1 μM) or protonophore carbonyl cyanide m-chlorophenyl hydrazone (CCCP, 1–3 μM) to evaluate how the membrane energy barrier is altered by RA-PE adducts. The results show that the barrier was decreased for the positive charge and increased for the negative charge when compared to the control without aldehydes (Fig. 3a). The effect of ONE on valinomycin was more pronounced than that of HNE. The decrease of the membrane energy barrier induced by aldehydes coincides with changes induced by the well-known dipole modifier, phloretin, under the same conditions (Fig. 3a, red bars) [36]. Since phloretin and RH421 decreases and increases membrane dipole potential, respectively, we added them to UCP-containing membranes to test the idea that the dipole potential (DP) change may be a mechanism responsible for the RA-mediated UCP activation. However, Fig. S10a–b shows that changes in conductance of membranes reconstituted with UCP1 and FA in the presence of two DP modifiers does not indicate the involvement of DP in the alteration of protein activity. It means that even if aldehydes change the dipole potential as a part of a boundary potential, it does not seem to be the molecular mechanism that affects UCP1 transport. In contrast, phloretin decreased the conductance of membranes reconstituted with arachidonic acid in a dose-dependent manner, whereas RH 421 increased it (Fig. S10c–d).

To evaluate whether a RA-mediated decrease of boundary potential may in part be explained by alteration of surface potential as previously described for calcium channel blocker verapamil [37], we compared the zeta-potential of liposomes composed of DOPC and of DOPC:DOPE (50:50 mol%). We have omitted CL from the lipid composition, because CL, as a strong anionic lipid, alters the surface potential itself. Ethanol (EtOH) and methyl acetate (MA) did not alter the zeta-potential. Our results show that RAs significantly increased negative membrane zeta-potential in the following order HHE < HNE≪ONE in DOPC:DOPE, but not in DOPC lipid bilayers (Fig. 3b).

Finally, we evaluated the influence of RAs on the order parameter, *S*, using an electron paramagnetic resonance technique (EPR) and 5-doxyl stearic acid. We compared the liposomes without additives (negative control), with AA (positive control [5]) and with different RAs and solvents (ethanol, MA). We found that only the incubation of liposomes with ONE lead to small but significant decreases in S for DOPC/DOPE liposomes (Fig. 3c; yellow bar). Again, we did not reveal any changes due to RA action in DOPC bilayers. These results indicate that modification of PE by ONE leads to the alteration in spatial arrangement of aliphatic chains in bilayers, and thus to an increase in the bilayers' fluidity. The PE-adducts formed by HNE and HHE do not modify the membrane order parameter.

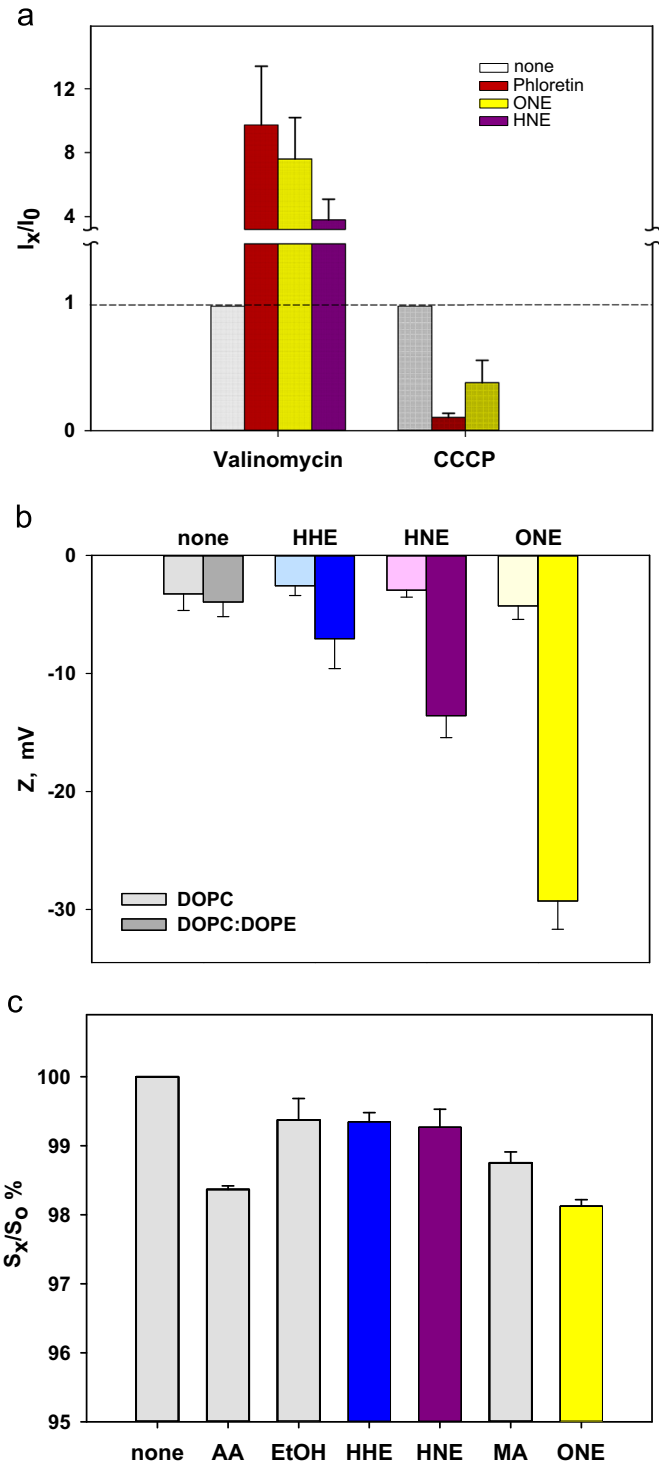

Fig. 3. Biophysical membrane parameters alteration by RAs. (a) Valinomycin- and CCCP-mediated membrane current measured in the presence (I_x) and absence (I_0) of ONE (yellow, 0.34 μM), HNE (violet, 0.32 μM) and phloretin (red, 5 and 80 μM). Membranes were made from DPhPC:DOPE (70:30 mol%). The buffer solution contained 50 mM KCl, 10 mM TRIS, 10 mM MES at pH 7.4 at T=25 °C. (b) Alteration of membrane surface potential due to interaction of RAs with DOPE. Liposomes were composed of DOPC: DOPE (50: 50, in mol%). Lipid concentration was 0.2 mg/ml. Concentrations of HHE, HNE and ONE were 0.5 mM. The buffer solution contained 50 mM Na_2SO_4, 10 mM TRIS, 10 mM MES, 0.6 mM EGTA at pH 7.35 at T=25 °C. (c) Order parameter in DOPE:DOPC membrane bilayer in the presence of reactive aldehydes and solvents. Liposomes contained DOPC:DOPE (50:50, in mol%). Concentration of liposomes was 5 mg/ml and of RAs was 0.5 mM. The concentration of the spin label 5-doxyl stearic acid (5-DSA) was 7.5 nmol/(mg lipid). S_0 was set to 100 and all other order parameters S_x were expressed in relation to this value. S_0 and S_x were measured with or without solvents (Ethanol, methyl acetate). The buffer solution and pH and T were as in B. Data points represent standard deviation from at least 3 independent experiments.

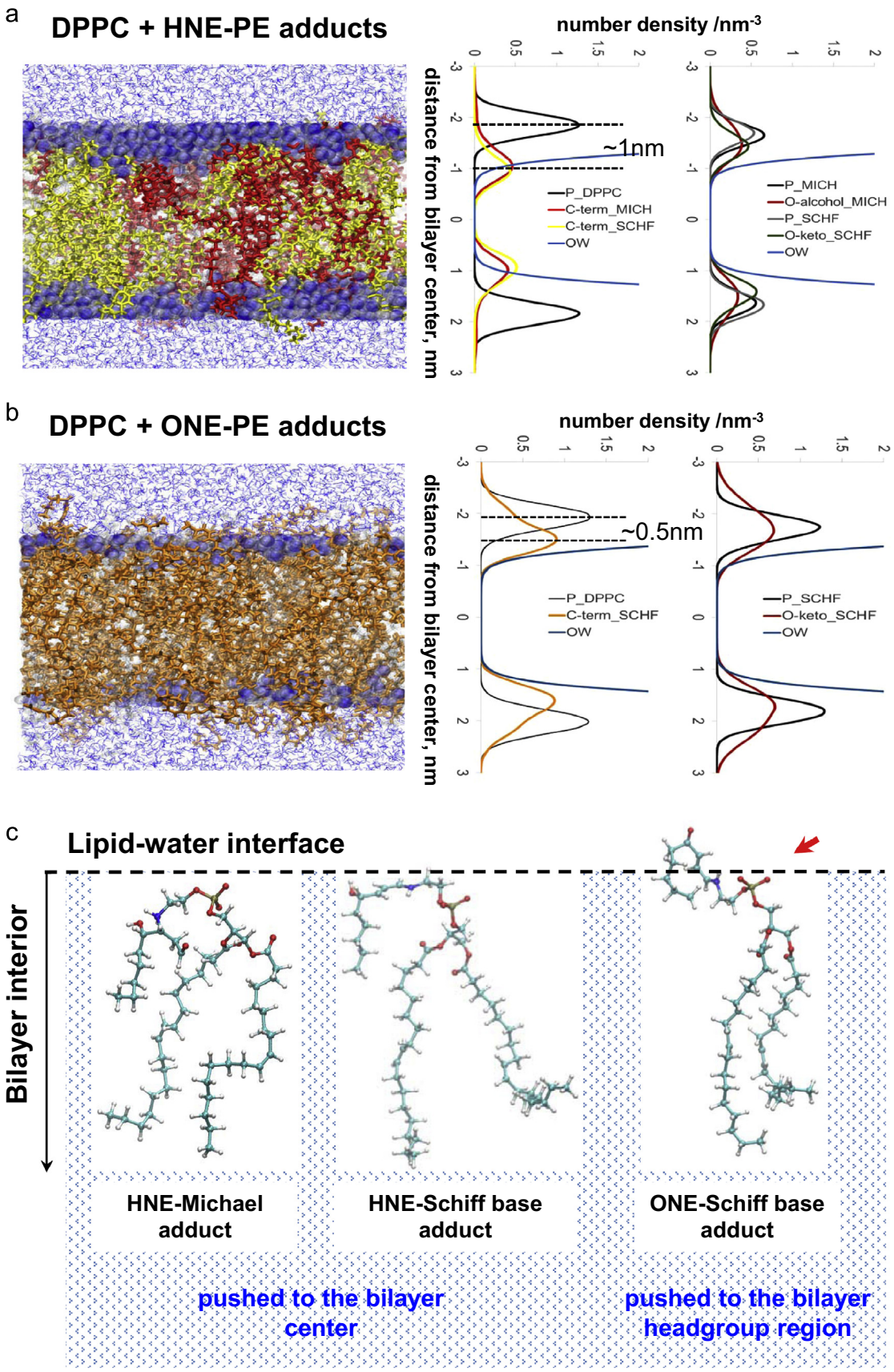

Fig. 4. Localization of (a) HNE-PE adducts and (b) ONE-Schiff adduct in DPPC bilayer (gray) revealed by molecular dynamics simulations (MD). Left column: selected MD snapshots, with HNE-Michael adduct in red, HNE-Schiff adduct in yellow and ONE-Schiff adduct in orange; middle column-number density profiles for the C terminus of RA/adducts (MICH and SCHF); right column- number density profiles for hydroxy (OH) and carbonyl (O) groups of RA/adducts. Water molecules inside the bilayer are shown in blue (OW); P_DPPC – phosphorus atom of DPPC, O-alcohol_MICH –alcohol group of Michael adduct. (c) Structural differences between HNE and ONE adducts influence their position in lipid bilayer membranes as revealed by MD simulations.

3.5. Molecular dynamics (MD) simulations of various lipid bilayer compositions

To understand how the RAs studied in the experimental part of this work alter properties of the lipid bilayer membrane, we performed MD simulations of DPPC bilayer with ONE, HNE, and RA-DOPE adducts (Fig. 4 and Figs. S11 and S12). The evaluation of number density profiles shows large qualitative differences between bilayers containing HNE adducts (both Michael and Schiff base adducts, Fig. 4a), and those containing only ONE Schiff base adducts (Fig. 4b). As indicated in Fig. 4b, the terminal carbon atom in the aliphatic tail of the ONE-Schiff base adducts (orange) is preferentially located close to the headgroup region with a density maximum at a distance of approximately 0.5 nm from the phosphorus atom (black) of the DPPC, which denotes the water–lipid interface. In contrast, the terminal carbon atoms of aliphatic tails of HNE-Michael adducts (red, Fig. 4a) and HNE-Schiff base adducts (yellow, Fig. 4a) are located deeper within the bilayer at a distance of approximately 1 nm from the phosphorus atom (black). Interestingly, the number density profiles of terminal carbon atoms for both HNE adducts, Michael and Schiff base adducts, overlap each other. It suggests great similarity between both adducts which results in their comparable position in lipid bilayers. Evidently the PE adducts which are formed by different RAs, diversely altered the lipid density profile in the bilayer as well: the ONE-Schiff base adducts contributed to an increase in lipid density in the headgroup region, whereas the HNE adducts increased the lipid density deeper into the region of aliphatic chains. The difference in the behavior of HNE and ONE adducts lies in their capability to form hydrogen bonds with DPPC phosphate and especially DPPC carbonyl groups which are located below the phosphate groups close to the aliphatic chain region. In particular, hydrogen bonds are readily formed between hydroxyl groups, present in HNE-Michael and HNE-Schiff adducts, with DPPC carbonyl groups which as a consequence results in the penetration of the adduct aliphatic tail deeper into the bilayer. In contrast, the carbonyl group in the ONE-Schiff adduct is not able to make hydrogen bonds with DPPC carbonyl groups, which in turn shifts the aliphatic tail closer to the water phase (Fig. 4c).

Analysis of the number density profiles shows that addition of ONE to the DPPC bilayer results in their stabilization in the lipid bilayer (Fig. S11), which is similar to what was previously demonstrated for HNE [38]. ONE increases the area per lipid by approximately 21%, similar to the effect of HNE on DPPC lipids (Fig. S12). Formation of ONE-PE adducts increased the area per lipid by only 8%, while formation of HNE-PE adducts increased the area per lipid by only 12%. The difference in area per lipid between HNE and ONE adducts is caused by the structural differences between these adducts as suggested in Fig. 4c. Interestingly, MD simulation did not show differences in area per lipid for HNE Michael adduct and HNE Schiff base adduct which once again indicates their great similarity in localization in lipid bilayer. Furthermore, the structural differences between HNE/ONE adducts and the different position of oxygen (arrow in Fig. 4c) could be the reason for the differences observed in surface potential measurements (Fig. 3b): oxygen in ONE-adducts is generally localized at the water–lipid region (Fig. 4b; right, red) in contrast to the oxygen in HHE- and HNE-adducts (Fig. 4a; right, red and green), which are mostly directed towards the membrane core.

4. Discussion

Biological effects on proteins mediated by HNE and ONE are usually attributed to their capacity to modify molecules by binding covalently to the nucleophilic sites such as cysteine, lysine and histidine (for review [6,33,39]). The ability of HNE to form Michael adducts with phosphatidylethanolamine (PE) was first suggested by Guichardant et al. [13]. Few studies have reported that other aldehydes also covalently bind to aminophospholipids, forming Michael and Schiff base adducts [14,40,41]. However, the consequences of such lipid modification for the function of membrane proteins and the type of adducts formed by different aldehydes have not yet been investigated. We have now demonstrated that the mechanism of aldehydes action on the transporter function is based on the formation of PE-aldehyde adducts, which for their part modify the biophysical properties of the membrane (Fig. 5). The mass spectrometry analysis revealed that all three RAs we examined, formed different adducts upon binding to the amino group of PE. In contrast to the previous work, in which only two HNE-derived adducts (Michael and Schiff base adducts) have been described [13], we have now showed that PE-HNE interaction results in the formation of four adducts including double Michael and Schiff base adducts. The amount of formed adducts obviously depends on the PE species and hydrophobicity of aldehydes as suggested in the study with isolated human blood platelets [14].

Notably, ONE, known as a most toxic aldehyde in cells [42], also revealed the most pronounced effect on conductance of bilayer membranes reconstituted with recombinant UCP1, valinomycin or CCCP. Since ONE forms merely one adduct with PE, we concluded that the formation of this ONE-Schiff base adduct may mainly be responsible for the activity change of studied transporters. In contrast, Michael, double Michael and Schiff base adducts formed by HNE and Michael adducts derived from HHE only moderately contributed to these changes. MD simulations reveal that structurally distinct PE adducts influence bilayer membrane properties in different ways. Thus, the increase of area per lipid is more pronounced in bilayers that contain both HNE adducts than those having only ONE Schiff base adduct. However, it seems to be more important that aliphatic chains of ONE Schiff adducts are located closer to the lipid headgroup region, in contrast to aliphatic chains of both Michael and Schiff HNE adducts which penetrate deeper into the bilayer interior. This fact suggests that the modification of the lipid headgroup position primarily led to the alteration of the transport properties of studied proteins.

The experimental data revealed that RA-PE adducts affect to different extent several membrane biophysical properties, such as boundary potentials and membrane order parameters, which in turn individually altered the function of each membrane transporter. ONE and to a lesser extent HNE decreased the positive membrane energy barrier that led to the increase of the potassium transport rate mediated by valinomycin. However, it does not seem to be the molecular mechanism which would explain the aldehyde action on mitochondrial transporter UCP1, because no effect on UCP1 function was observed in the presence of dipole potential modifiers phloretin and RH 421 (Fig. S10). We suggest that an increase in UCP1-mediated conductance rather depends on membrane fluidity and/or membrane surface potential, as previously shown for UCP2 in the presence of negatively charged phosphoinositides [43]. These mechanisms would be conform with the view that fatty acids, known as activators of UCP1 transport, bind to the protein on the protein–lipid surface as suggested by the FA-cycling hypothesis and in the subsequent works [44,45].

Based on the presented data we hypothesized that the shown PE-mediated mechanism of RA action is not specific for UCP1, but can be common for all membrane proteins. This hypothesis is already supported in the present work by data demonstrating that the activity of a small membrane transporter valinomycin is affected by PE-adducts through the boundary potential alteration. To test this hypothesis further experiments with other membrane proteins are required.

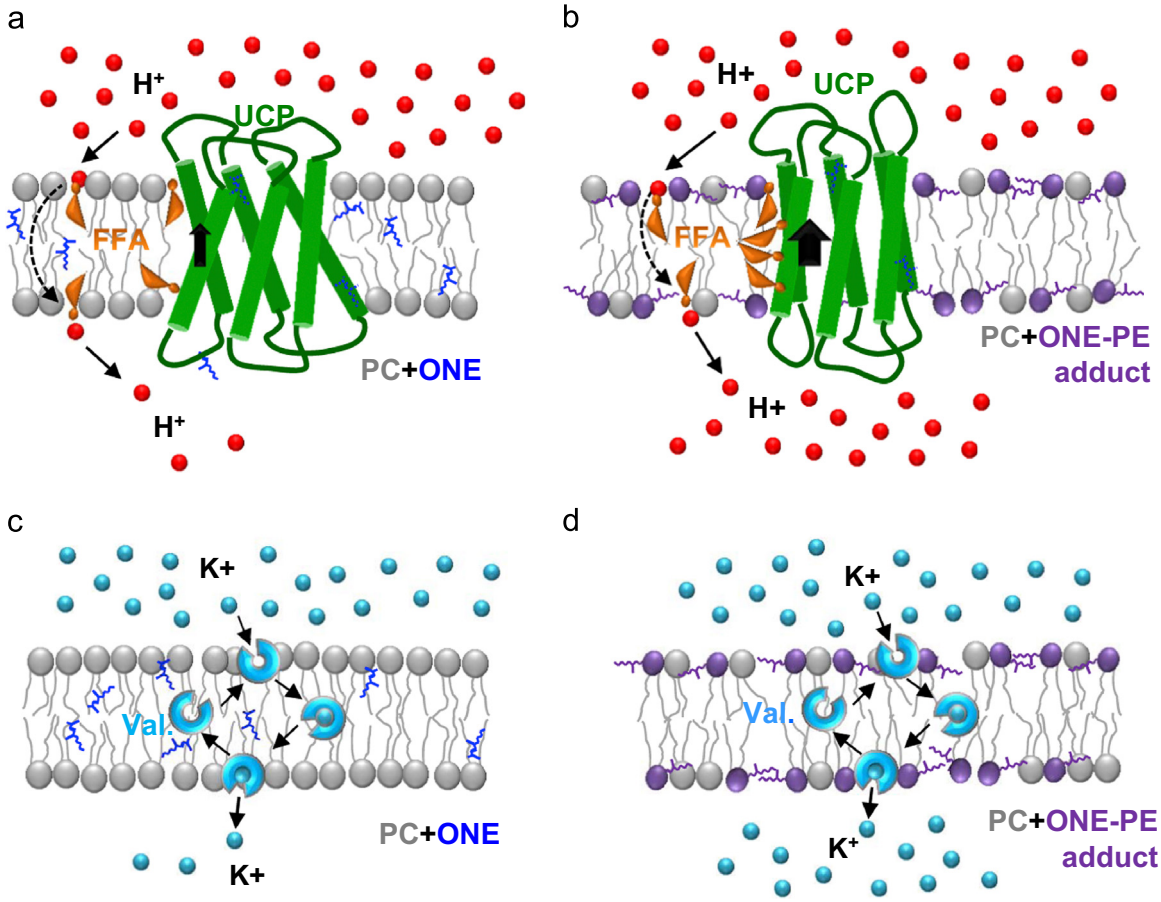

Fig. 5. Mechanism of aldehyde action on transmembrane transporters in PE-free (left column) and PE-containing bilayers (right column). UCP-mediated proton translocation in the presence of free fatty acids (FFAs) and valinomycin-mediated K^+ transport are faster in bilayers containing RA-PE adducts (b, d) than in PC bilayers, containing ONE (a, c).

5. Conclusion

Our results show that at least two molecular mechanisms can explain the action of aldehydes on proteins or peptides at cellular level. On the one side, RAs may directly modify protein conformation or function by binding to several positively charged amino acids. On the other side, aldehydes form different adducts with PE which led to the alteration of membrane properties and finally to the modification of protein function. Whereas the first mechanism may be more relevant for hydrophilic proteins, the second mechanism seems to be crucial for membrane proteins. Membrane lipid asymmetry and PE abundance in the membrane may thereby play a regulatory role. The aldehyde´s ability to affect the molecules by different mechanisms would explain the diversity of aldehyde effects observed in cells and their involvement in the onset and progression of many diseases.

Notes

The authors declare that they have no competing financial interest.

Acknowledgments

This work was supported by the Austrian Research Fund (FWF, P25123 to E.P.), the European Regional Development Fund (ERDF, European Union and Free State Saxony; 100146238 and 100121468 to M.F). We thank Dr. Anne Rupprecht (University of Veterinary Medicine, Vienna) for the production of recombinant proteins and Pr. Ralf Hoffmann (Institute of Bioanalytical Radical Chemistry, University of Leipzig) for providing access to his laboratory and mass spectrometers. The authors are grateful to COST Action CM1201 Biomimetic Radical Chemistry for the scientific exchange and cooperation. We thank Quentina Beatty for editorial assistance.

Appendix A. Supplementary material

Supplementary data associated with this article can be found in the online version at http://dx.doi.org/10.1016/j.freeradbiomed.2015.10.422.

References

[1] A. Catala, Lipid peroxidation of membrane phospholipids generates hydroxy-alkenals and oxidized phospholipids active in physiological and/or pathological conditions, Chem. Phys. Lipids 157 (2009) 1–11.
[2] E.K. Long, M.J. Picklo Sr., Trans-4-hydroxy-2-hexenal, a product of n-3 fatty acid peroxidation: make some room HNE, Free Radic. Biol. Med. 49 (2010) 1–8.
[3] H. Esterbauer, R.J. Schaur, H. Zollner, Chemistry and biochemistry of 4-hydroxynonenal, malonaldehyde and related aldehydes, Free Radic. Biol. Med. 11 (1991) 81–128.
[4] J.R. Roede, D.P. Jones, Reactive species and mitochondrial dysfunction: mechanistic significance of 4-hydroxynonenal, Environ. Mol. Mutagen. 51 (2010) 380–390.
[5] E.A. Malingriaux, A. Rupprecht, L. Gille, O. Jovanovic, P. Jezek, M. Jaburek, et al., Fatty acids are key in 4-hydroxy-2-nonenal-mediated activation of uncoupling

proteins 1 and 2, PLoS One 8 (2013) e77786.
[6] N. Zarkovic, A. Cipak, M. Jaganjac, S. Borovic, K. Zarkovic, Pathophysiological relevance of aldehydic protein modifications, J. Proteom. 92 (2013) 239–247.
[7] J.J. Galligan, K.L. Rose, W.N. Beavers, S. Hill, K.A. Tallman, W.P. Tansey, et al., Stable histone adduction by 4-oxo-2-nonenal: a potential link between oxidative stress and epigenetics, J. Am. Chem. Soc. 136 (2014) 11864–11866.
[8] L. Milkovic, G.A. Cipak, N. Zarkovic, Overview on major lipid peroxidation bioactive factor 4-hydroxynonenal as pluripotent growth regulating factor, Free Radic. Res.49 (2015) 850–860.
[9] G. Poli, R.J. Schaur, W.G. Siems, G. Leonarduzzi, 4-hydroxynonenal: a membrane lipid oxidation product of medicinal interest, Med. Res. Rev. 28 (2008) 569–631.
[10] G. Poli, F. Biasi, G. Leonarduzzi, 4-Hydroxynonenal-protein adducts: a reliable biomarker of lipid oxidation in liver diseases, Mol. Asp. Med. 29 (2008) 67–71.
[11] G. Barrera, S. Pizzimenti, E.S. Ciamporcero, M. Daga, C. Ullio, A. Arcaro, et al., Role of 4-hydroxynonenal-protein adducts in human diseases, Antioxid. Redox Signal. 22 (2015) 1681–1702.
[12] R. Pamplona, Advanced lipoxidation end-products, Chem. Biol. Interact. 192 (2011) 14–20.
[13] M. Guichardant, P. Taibi-Tronche, L.B. Fay, M. Lagarde, Covalent modifications of aminophospholipids by 4-hydroxynonenal, Free Radic. Biol. Med. 25 (1998) 1049–1056.
[14] S. Bacot, N. Bernoud-Hubac, N. Baddas, B. Chantegrel, C. Deshayes, A. Doutheau, et al., Covalent binding of hydroxy-alkenals 4-HDDE, 4-HHE, and 4-HNE to ethanolamine phospholipid subclasses, J. Lipid Res. 44 (2003) 917–926.
[15] N. Parker, A. Vidal-Puig, M.D. Brand, Stimulation of mitochondrial proton conductance by hydroxynonenal requires a high membrane potential, Biosci. Rep. 28 (2008) 83–88.
[16] I.G. Shabalina, N. Petrovic, T.V. Kramarova, J. Hoeks, B. Cannon, J. Nedergaard, UCP1 and defense against oxidative stress. 4-Hydroxy-2-nonenal effects on brown fat mitochondria are uncoupling protein 1-independent, J. Biol. Chem. 281 (2006) 13882–13893.
[17] A. Rupprecht, E.A. Sokolenko, V. Beck, O. Ninnemann, M. Jaburek, T. Trimbuch, et al., Role of the transmembrane potential in the membrane proton leak, Biophys. J. 98 (2010) 1503–1511.
[18] V. Beck, M. Jaburek, E.P. Breen, R.K. Porter, P. Jezek, E.E. Pohl, A new automated technique for the reconstitution of hydrophobic proteins into planar bilayer membranes. Studies of human recombinant uncoupling protein 1, Biochim. Biophys. Acta 1757 (2006) 474–479.
[19] A. Bolognesi, A. Chatgilialoglu, L. Polito, C. Ferreri, Membrane lipidome reorganization correlates with the fate of neuroblastoma cells supplemented with fatty acids, PLoS One 8 (2013) e55537.
[20] J.P. Jämbeck, A.P. Lyubartsev, Derivation and systematic validation of a refined all-atom force field for phosphatidylcholine lipids, J. Phys. Chem. B 116 (2012) 3164–3179.
[21] J.P. Jämbeck, A.P. Lyubartsev, An extension and further validation of an all-atomistic force field for biological membranes, J. Chem. Theory Comput. 8 (2012) 2938–2948.
[22] J.P. Jämbeck, A.P. Lyubartsev, Another piece of the membrane puzzle: extending slipids further, J. Chem. Theory Comput. 9 (2012) 774–784.
[23] J.B. Klauda, R.M. Venable, J.A. Freites, J.W. O'Connor, D.J. Tobias, C. Mondragon-Ramirez, et al., Update of the CHARMM all-atom additive force field for lipids: validation on six lipid types, J. Phys. Chem. B 114 (2010) 7830–7843.
[24] W.L. Jorgensen, J. Chandrasekhar, J.D. Madura, R.W. Impey, M.L. Klein, Comparison of simple potential functions for simulating liquid water, J. Chem. Phys. 79 (1983) 926–935.
[25] U.C. Singh, P.A. Kollman, An approach to computing electrostatic charges for molecules, J. Comput. Chem. 5 (1984) 129–145.
[26] U. Essmann, L. Perera, M.L. Berkowitz, T. Darden, H. Lee, L.G. Pedersen, A smooth particle mesh Ewald method, J. Chem. Phys. 103 (1995) 8577–8593.
[27] M. Parrinello, A. Rahman, Polymorphic transitions in single crystals: a new molecular dynamics method, J. Appl. Phys. 52 (1981) 7182–7190.
[28] S. Nose, A molecular dynamics method for simulations in the canonical ensemble, Mol. Phys. 52 (1984) 255–268.
[29] B. Hess, H. Bekker, H.J. Berendsen, J.G. Fraaije, LINCS: a linear constraint solver for molecular simulations, J. Comput. Chem. 18 (1997) 1463–1472.
[30] R.W. Hockney, S.P. Goel, J.W. Eastwood, Quiet high-resolution computer models of a plasma, J. Comput. Phys. 14 (1974) 148–158.
[31] B. Hess, C. Kutzner, D. Van Der Spoel, E. Lindahl, GROMACS 4: algorithms for highly efficient, load-balanced, and scalable molecular simulation, J. Chem. Theory Comput. 4 (2008) 435–447.
[32] M.J. Frisch, G.W. Trucks, H.B. Schlegel, G.E. Scuseria, M.A. Robb, J.R. Cheeseman, Gaussian 09, Revision A. 1., Gaussian Inc., Wallingford, CT, 2009.
[33] L.M. Sayre, D. Lin, Q. Yuan, X. Zhu, X. Tang, Protein adducts generated from products of lipid oxidation: focus on HNE and one, Drug Metab. Rev. 38 (2006) 651–675.
[34] L. Guo, Z. Chen, V. Amarnath, S.S. Davies, Identification of novel bioactive aldehyde-modified phosphatidylethanolamines formed by lipid peroxidation, Free Radic. Biol. Med. 53 (2012) 1226–1238.
[35] A. Annibal, K. Schubert, U. Wagner, R. Hoffmann, J. Schiller, M. Fedorova, New covalent modifications of phosphatidylethanolamine by alkanals: mass spectrometry based structural characterization and biological effects, J. Mass. Spectrom. 49 (2014) 557–569.
[36] P. Pohl, T.I. Rokitskaya, E.E. Pohl, S.M. Saparov, Permeation of phloretin across bilayer lipid membranes monitored by dipole potential and microelectrode measurements, Biochim. Biophys. Acta 1323 (1997) 163–172.
[37] E.E. Pohl, A.V. Krylov, M. Block, P. Pohl, Changes of the membrane potential profile induced by verapamil and propranolol, Biochim. Biophys. Acta: Biomembr. 1373 (1998) 170–178.
[38] M. Vazdar, P. Jurkiewicz, M. Hof, P. Jungwirth, L. Cwiklik, Behavior of 4-hydroxynonenal in phospholipid membranes, J. Phys. Chem. B 116 (2012) 6411–6415.
[39] S. Pizzimenti, E. Ciamporcero, M. Daga, P. Pettazzoni, A. Arcaro, G. Cetrangolo, et al., Interaction of aldehydes derived from lipid peroxidation and membrane proteins, Front. Physiol. 4 (2013) 242.
[40] N. Bernoud-Hubac, L.B. Fay, V. Armarnath, M. Guichardant, S. Bacot, S. S. Davies, et al., Covalent binding of isoketals to ethanolamine phospholipids, Free Radic. Biol. Med. 37 (2004) 1604–1611.
[41] S. Bacot, N. Bernoud-Hubac, B. Chantegrel, C. Deshayes, A. Doutheau, G. Ponsin, et al., Evidence for in situ ethanolamine phospholipid adducts with hydroxy-alkenals, J. Lipid Res. 48 (2007) 816–825.
[42] D. Lin, H.G. Lee, Q. Liu, G. Perry, M.A. Smith, L.M. Sayre, 4-Oxo-2-nonenal is both more neurotoxic and more protein reactive than 4-hydroxy-2-nonenal, Chem. Res. Toxicol. 18 (2005) 1219–1231.
[43] W.M. Yu, X. Liu, J. Shen, O. Jovanovic, E.E. Pohl, S.L. Gerson, et al., Metabolic regulation by the mitochondrial phosphatase PTPMT1 is required for hematopoietic stem cell differentiation, Cell Stem Cell 12 (2013) 62–74.
[44] V.P. Skulachev, Fatty acid circuit as a physiological mechanism of uncoupling of oxidative phosphorylation, FEBS Lett. 294 (1991) 158–162.
[45] K.D. Garlid, D.E. Orosz, M. Modriansky, S. Vassanelli, P. Jezek, On the mechanism of fatty acid-induced proton transport by mitochondrial uncoupling protein, J. Biol. Chem. 271 (1996) 2615–2620.